Asteroid Deflection Theory: fundamentals of orbital mechanics and optimal control

D. Izzo, J. Olympio , C. H. Yam[(1)]

[(1)] ***ESA, Advanced Concepts Team, ESTEC, Keplerlaan 1, Postbus 299, 2200 AG, Noordwijk***
E-mail address: dario.izzo@esa.int

Abstract

The problem of artificially changing the orbit of an asteroid to avoid possible future impacts is discussed from the orbital mechanics point of view. We study the accuracy of analytical estimates for the encounter b-plane displacement of the asteroid. Based on these estimates we introduce the deflection charts as a way to preliminary assess an asteroid threat and select possible deflection options. We then discuss the asteroid deflection optimal control problem as a mean to perform a precise assessment of a given deflection threat. We show how the outcome of trade-offs between deflection strategies depend on the spacecraft design and on the asteroid-Earth phasing.

Nomenclature

$\Delta\mathbf{V}$	Impulsive velocity change vector applied to the asteroid
$\Delta\zeta$	Displacement on the encounter b-plane of the asteroid image.
Δr	Magnitude of the change, at encounter, in the heliocentric asteroid position due to the deflection.
λ_m	Costate of the mass
$\mathbf{A}$	Deflection acceleration.
$\mathbf{U}_{ast}$	Asteroid unperturbed velocity relative to the Earth at encounter.
$\chi(\mathbf{t_L})$	Decision vector
λ_R	Costate of the position
λ_V	Costate of the velocity
$\mathbf{f}(\mathbf{x},\mathbf{u};t)$	Spacecraft dynamic function
$\mathbf{r}_{ast}$	Asteroid unperturbed heliocentric position.
$\mathbf{r}_{sc}$	Spacecraft position
$\mathbf{u}$	Spacecraft control
$\mathbf{v}_{ast}$	Asteroid unperturbed heliocentric velocity.
$\mathbf{v}_{sc}$	Spacecraft velocity
$\mathbf{x}$	Spacecraft state vector
μ	Gravitational parameter of the Sun
$\pi_.$	Transversality conditions
$\psi_.$	State constraints
τ	Time from deflection start.
τ_p	Push time.
τ_s	Start time. This is also the Earth encounter Epoch in the new time axis.
θ	The angle between $\mathbf{v}_{E,t_e}$ and $\mathbf{U}_{ast}$.
a	Asteroid semi-major axis
F_{Th}	Maximum spacecraft thrust
g_0	Standard gravity
I_{Sp}	Spacecraft Thruster Specific Impulse

m_{sc}	Spacecraft mass
t_0	Impulse epoch or, later, the epoch of the spacecraft arrival to the asteroid
t_e	Earth encounter Epoch
t_L	Spacecraft Launch Epoch
v_E	Earth heliocentric velocity.

Introduction

The artificial modification of an asteroid orbit for deflection purposes is a technological challenge that scientists are taking more and more seriously as our knowledge on the Near Earth Objects population is improving. It is becoming increasingly clear that asteroids do cause natural disasters of different magnitudes and with different (and fortunately low) frequencies and that these are the only type of natural disasters that we can actively prevent from happening. This requires an early detection of the hazardous object, an assessment of the risk posed and a subsequent mitigation action. While the three steps are equally important, we here concentrate on the last and in particular on those cases where the only possible mitigation action is to deflect the asteroid. Our aim in this paper is to study the "dynamics of moving asteroids" [1] intended as the study of the asteroid orbit perturbed by artificially induced external accelerations. Such a subject allows for simplifications to the methods traditionally used in the study of the dynamic of spacecraft trajectories, as the magnitude of the acceleration we can optimistically hope to artificially induce on an asteroid is extremely small when compared to the acceleration level of a spacecraft equipped with low-thrust propulsion. This simple fact make the nonlinearities in orbital mechanics almost disappear. In the early work of Ahrens and Harris (1992) [2] elementary orbital dynamic formulas are used to show that impulsive velocity increments resulting in changes to the asteroid semi-major axis allow, for long enough warning times, a larger effect with respect to velocity increments resulting in changes to the asteroid eccentricity and inclination. Valsecchi et al. (2001) introduce ζ as the b-plane coordinate function only of the difference in timing between the asteroid and the Earth. Using this coordinate, Carusi et al. [3] published a refinement to Ahrens and Harris work in the form of a compact formula relating the impulsive velocity increment magnitude (assumed to be along the asteroid velocity vector) to the required displacement along the ζ axis. The work of Kahle et al. (2006) [4] present a numerical method able to extend this expression to arbitrary direction velocity increments, while Rathke and Izzo (2007) [5] obtain similar results using an analytical approach. A few years before, Scheeres et al. (2004) [1] had started to consider the same problem for non-impulsive velocity increments showing that analytical results were still possible in this case. Eventually, Izzo (2006) [6] obtained one compact expression, the asteroid deflection formula, valid for deflection acceleration along the velocity vector and showed its reduction to previously obtained results using simple calculations. Along these research lines, in this paper, we take a few steps further showing the use of the deflection formula in the preliminary assessment of the deflection capability of a certain deflection strategy. We then argue its use in the the optimal control problem arising in the spacecraft trajectory design of a deflection mission presenting a few results on the optimal control structure of the control in these unusual cases. We finally apply our results to a case study: the trade-off between a kinetic impactor and a gravity tractor strategy for the case of the asteroid Apophis.

Impulsive Deflection

Consider an asteroid following a keplerian orbit. We indicate its heliocentric position and velocity with the variables $\mathbf{r}_{ast}$ and $\mathbf{v}_{ast}$. At the epoch t_0 we apply an impulsive velocity change $\Delta\mathbf{V}$ and observe its change in position $\Delta\mathbf{r}$ at the next Earth encounter at time t_e. Rathke and Izzo [5] developed a full expression of $\Delta\mathbf{r}$ using the variation of parameter method [7]. Here we will only use the secular term of that expression for the heliocentric deflection distance Δr [3] [6] defined as:

$$\Delta r = \frac{3a}{\mu} v_{ast,t_e}(t_e - t_0)(\mathbf{v}_{ast,t_0} \cdot \Delta\mathbf{V}) \tag{1}$$

An expression of the $\Delta V_{||}$ to apply along the asteroid velocity (i.e., tangential) in order to obtain a fixed deflection Δr, can be found by substituting v_{ast} with $\sqrt{\mu\,(2a - r_{ast})\,/\,(ar_{ast})}$, which gives:

$$\Delta V_{||} = \frac{\Delta r \sqrt{r_{ast,t_e} r_{ast,t_0}}}{3(t_e - t_0)\sqrt{2a - r_{ast,t_e}}\sqrt{2a - r_{ast,t_0}}} \tag{2}$$

We can use Eq.(2) to estimate the required ΔV for a given deflection distance, at any time t_0 along the asteroid's orbit. An example is illustrated in Fig. (1) for the asteroid Apophis. We note that even with a

simple formula and two-body propagation, results shown in Fig. (1) have very similar trends as compared to the work found by n-body simulation[3][8]. The two curves shown in the figure are calculated from Eq.(2), labeled as *Analytical*, and an iterative two-body numerical simulation, labeled as *Numerical*. The results are found in two steps: (1) To deflect the asteroid outside the keyhole, from the year 2010 to April 2029, Δr is assumed to be 1 km as the keyhole size of Apophis is known to be 600 m [8]. (2) To avoid an impact in April 2036, the deflection distance is set to be equal to the Earth radius amplified by the focusing factor. The jump in the ΔV after encounter in 2029 can be explained by the increase in the required Δr of 4 orders of magnitude. The orbital parameters of Apophis after the 2029 encounter are chosen such that its orbital period becomes 7.0 years and keeping the closest distance with the Earth during the 2029 hyperbola to about 32,000 km.

The two-body numerical simulation in Fig. (1) assumes a tangential ΔV. We present a second scenario where the direction of the ΔV is allowed to changed in its orbital plane. Various ΔV angles (measured from its current velocity vector) are considered along the same interception time frame. For each t_0, an optimal angle is selected in which the ΔV required is minimum to achieve the same deflected distance Δr. From Fig. (2), we note that for most of the time, the optimal ΔV direction remains very close to be tangential and the difference between tangential and optimal ΔV is very small, except when the asteroid approaches the Earth for its final heliocentric revolution.

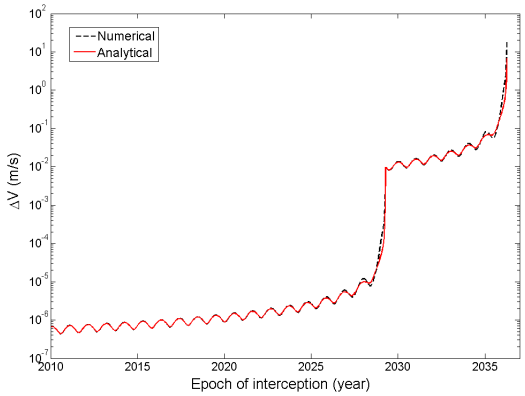

Figure 1: $\Delta\mathbf{V}$ required to deflect Apophis as a function of the epoch of interception.

Generic Deflection

We now consider the asteroid being accelerated away from its reference orbit by a deflection acceleration $\mathbf{A}(t)$ acting continuously over the time interval $[t_0, t_0 + \tau_p]$. We introduce, following Scheeres [1], a new time axis $\tau = t - t_0$. The duration of the deflection acceleration will thus be τ_p, or push time, and $\tau_s = t_e - t_0$, or start time, will represent the time before impact the deflection starts (and, in this new time axis, also the Earth encounter epoch). We approximate the deflection acceleration with a series of N impulses $\mathbf{A}(\tau) \approx \sum_{i=1}^{N} \Delta\mathbf{V}_i \delta(\tau - \frac{i}{N}\tau_p)$, where $\Delta\mathbf{V}_i = \int_{\frac{i-1}{N}\tau_p}^{\frac{i}{N}\tau_p} \mathbf{A}(\tau) d\tau$. The heliocentric deflection Δr will be the sum of the contributions due to each one of the impulses $\Delta r = \sum_{i=1}^{N} \Delta r_i$. Clearly, to use Eq.(1) to evaluate each contribution, one has to change the reference orbit after each velocity increment (i.e new a and $\mathbf{v}_{ast}$). On the other hand, in foreseeable deflection scenarios, such a change will be exceedingly small and will thus be neglected. In this case the contribution of each $\Delta\mathbf{V}_i$ to the final heliocentric deflection can be evaluated independently of all the others using Eq.(1). Following this ansaz and recovering the continuous representation of the deflection action $\mathbf{A}$ taking the limit for $N \to \infty$ we reach the following expression for the heliocentric deflection vector:

$$\Delta r = -\frac{3 a v_{ast,t_e}}{\mu} \int_0^{\tau_p} [\mathbf{v}(\tau) \cdot \mathbf{A}(\tau)] d\tau \,, \tag{3}$$

Projecting this expression on the encounter b-plane, we have:

$$\Delta\zeta = -\frac{3 a v_{E,t_e} \sin\theta}{\mu} \int_0^{\tau_p} (\tau_s - \tau)[\mathbf{v}(\tau) \cdot \mathbf{A}(\tau)] d\tau \,, \tag{4}$$

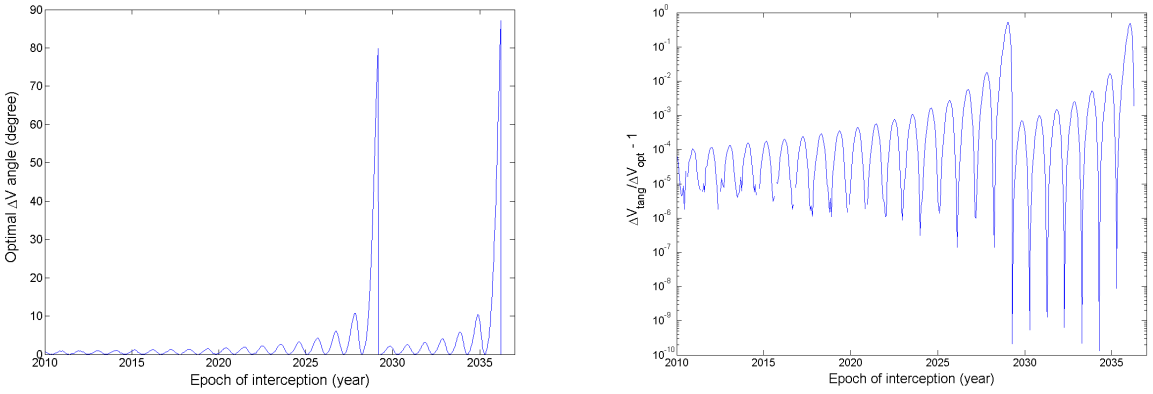

(a) Optimal impact angle

(b) Relative difference between tangential and and optimal impacts

Figure 2: Apophis deflection using a kinetic impactor

where θ represents the angle between the Earth velocity at encounter $\mathbf{v}_{E,t_e}$ and the asteroid relative velocity $\mathbf{U}_{ast}$ at encounter and $\Delta\zeta$ measures the displacement of the asteroid image on the encounter b-plane due to the deflection acceleration $\mathbf{A}$. Several properties of this last equations (also called the asteroid deflection formula) are detailed in a previous work [6] where its accuracy is also studied numerically for a few interesting cases that demonstrate its use for practical applications. It is noteworthy to remind that Eq.(4) reduces to previously published results (i.e. Carusi et al. [3] and Scheerers and Schweighart [1]) when introducing further assumptions (see [6]).

Deflection Charts

The asteroid deflection formula allows us to introduce a new type of charts that are useful to preliminary assess the threat of a given impact scenario. These are essentially a contour plot of Eq.(4) with $A = \frac{1}{m_{ast}}\mathbf{i}_v$ (i.e. deflection acceleration aligned with the asteroid velocity). Under these assumption the b-plane deflection is a sole function of τ_s and τ_p, that is of the start and the push times.
In Figure 3(a) the deflection chart relative to the 99942 Apophis close encounter in 2029 is shown. In Figure 3(b) we have reported the deflection chart for the asteroid 2009 KK and its close Earth encounter in 2022. The amount of deflection on the encounter b-plane that can be achieved by pushing constantly along the asteroid heliocentric velocity vector with a $1N$ force is plotted. As the two asteroids have a similar estimated mass ($m_{apo} = 2.7 \cdot 10^{10}$, $m_{kk} = 2.6 \cdot 10^{10} kg$) the order of magnitudes of the deflection achievable are quite similar, but the trend with respect to the variables τ_s and τ_p are different. The deflection charts are useful to preliminary assess the capabilities of a putative deflection mission aimed at moving the asteroid b-plane uncertainty ellipsoid out of dangerous areas. The linear behavior of $\Delta\zeta$ with respect to A and m_{ast} allows also to use the charts to quantify the sensitivity to these parameters of the achievable deflection. The charts also show clearly how the correct combination of τ_s and τ_p is critical to obtain the best possible deflection. Consider the case of a spacecraft that arrives at the asteroid 2009 KK 8.13 years before its Earth close encounter. Assume that the spacecraft is capable to push the asteroid for a period of 0.82 years and that it starts the deflection action immediately after its arrival (upper dot in Figure 3(b)). Such an intuitive strategy would, though, be far from optimal as the same spacecraft could wait three years before starting to push and with only 0.72 years of push would achieve three times as much deflection. Such a case is frequent for asteroid with high eccentricity orbits where the orbital velocity has a great variability and thus the efficiency of our push changes significantly if we operate at its aphelion or at its perihelion. Complex cases could force us to consider switching on and off the engines along multiple asteroid orbits. The deflection formula can be used also in these cases to perform a simple optimization of the thrust arcs once τ_s is given. The limits of this methodology is that it assumes implicitly that the spacecraft can reach the asteroid as easily at any given time disregarding the phasing between the Earth (from where the spacecraft is launched). Some arrival dates could just be infeasible for a given spacecraft, or could require so much fuel that little would be left at arrival to actually push the asteroid (for some deflection strategies such as the gravity tractor the propellant available on board at arrival is used to produce the deflection action). In general, a more accurate estimate of the deflection capabilities of a given spacecraft requires to consider the concurrent

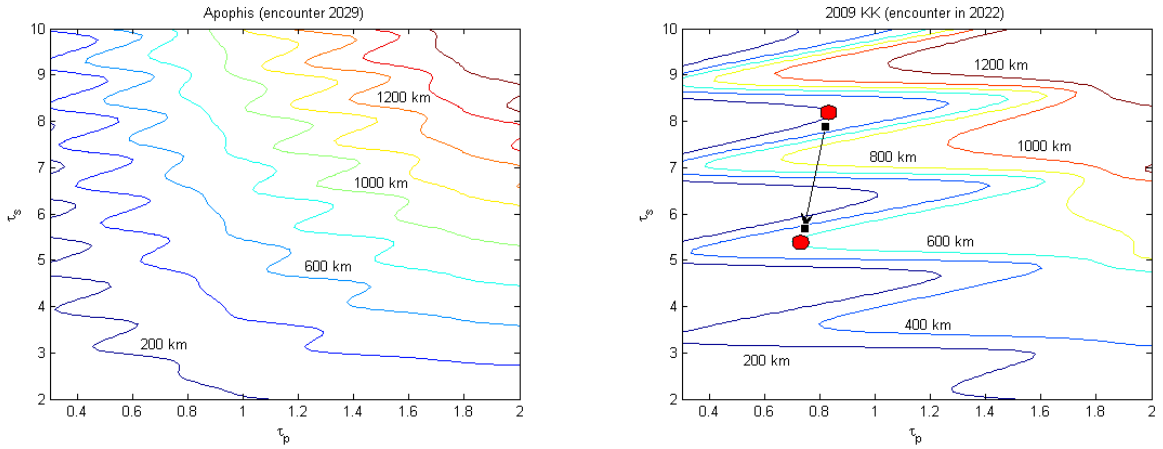

(a) Small e (b) Big e

Figure 3: Deflection charts for two different asteroids having a small and a big eccentricity. On (b) the red dots explain the counter-intuitive case of a spacecraft having to wait before starting its deflection action in order to maximize the deflection action.

optimization of the interplanetary trajectory and of τ_s and τ_p. This can be done by considering an optimal control problem for the spacecraft thrust where the objective function is given by Eq.(4). Such an unusual objective function (essentially depending on both the transfer duration and the spacecraft final mass) is considered in the following sections in the framework of indirect methods for trajectory optimization.

The Optimal Control Problem for asteroid deflection

Problem Statement

In a mitigation mission, the first part of the mission is the launch and the asteroid encounter phase. In this section, we propose results on the optimal control to place the spacecraft in a given state, to maximise the asteroid deflection. We study the transfer problem from Earth to the asteroid, a two-body problem and the sun is the only attracting body. We assume the departure and arrival date are fixed as we will grid sample later on these variables. We describe the state vector $\mathbf{x}$ of a spacecraft with its position $\mathbf{R}_{sc}$ and velocity $\mathbf{V}_{sc}$ in the heliocentric reference frame, and with its mass m_{sc}, . We introduce the dynamics:

$$\mathbf{f}(\mathbf{x},\mathbf{u};t) = \begin{bmatrix} \mathbf{V}_{sc}(t) \\ -\mu\frac{\mathbf{R}_{sc}(t)}{\|\mathbf{R}_{sc}(t)\|^3} + \frac{F_{Th}}{m_{sc}(t)}\mathbf{u}(t) \\ -\frac{F_{Th}}{g_0 I_{sp}}\|\mathbf{u}(t)\| \end{bmatrix} \tag{5}$$

To account for the initial position of the spacecraft, and the desired terminal state at the time of encounter, we introduce initial conditions and constraint. The initial conditions,

$$\begin{bmatrix} \mathbf{R}_{sc}(t_L) - \mathbf{R}_E(t_L) \\ m_{sc}(t_L) - m_0 \end{bmatrix} = 0 \tag{6}$$

and the initial constraints,

$$\psi_0(\mathbf{x};t_L) = \|\mathbf{V}_{sc}(t_L) - \mathbf{v}_E(t_L)\| - V_\infty \tag{7}$$

with $V_\infty = \|\mathbf{V}_{sc}(t_L) - \mathbf{v}_E(t_L)\|$. The initial constraint states that the spacecraft is launched from Earth, with a fixed launch energy $C_3 = V_\infty^2$.

For generality with further developement, we pose for now the general formulation for the terminal constraints:

$$\psi_f(\mathbf{x};t_0) = 0 \tag{8}$$

Because we consider two-body dynamics, and in the absence of capturing effects, the terminal constraints change from case to case. In the kinetic impactor case we are only interested in satisfying the encounter position with the asteroid, while in a gravity tractor case, we have to hover the asteroid and thus we might

consider a rendezvous constraint. We assume a spacecraft using an electric propulsion system. As such, the thrust can vary but is bounded to the maximum value F_{Th}. We introduce then the dynamic control constraint,

$$\|\mathbf{u}(t)\| \leq 1 \tag{9}$$

The problem is to minimise the objective function, or performance index, $J = -\Delta\zeta$, where the deflection $\Delta\zeta$ is given by Eq.(4).

Optimal Control

Consider the objective function and constraints just described, we are seeking the control that minimises the objective function J . We introduce costate vectors $\lambda_{\mathbf{R}}(t)$, $\lambda_{\mathbf{V}}(t)$ and $\lambda_m(t)$ associated respectively to $\mathbf{R}(t)$, $\mathbf{V}(t)$ and $m(t)$, and the Lagrange multipliers ν_0 and ν_f, to augment the performance index, such as,

$$L = J + \int_{t_L}^{t_0} \lambda(t)^T \left(\frac{d\mathbf{x}}{dt} - \mathbf{f}(\mathbf{x}, \mathbf{u}; t) \right) dt + \nu_f^T \psi_f(\mathbf{x}; t_0) + \nu_0 \psi_0(\mathbf{x}; t_L) \tag{10}$$

with $\lambda(t)^T = [\lambda_{\mathbf{R}}(t)^T, \lambda_{\mathbf{V}}(t)^T, \lambda_m(t)]$. We can then introduce the Hamiltonian,

$$H(\mathbf{x}, \lambda, \mathbf{u}; t) = [\lambda_{\mathbf{R}}(t)^T, \lambda_{\mathbf{V}}(t)^T, \lambda_m(t)]\mathbf{f}(\mathbf{x}, \mathbf{u}; t) \tag{11}$$

The necessary conditions of optimality can be found stating the stationarity of the Lagrangian L of the optimisation problem. This leads then to the well-known Euler-Lagrange equations, which describe the dynamics of the costate vectors,

$$\begin{cases} \dfrac{d\mathbf{x}}{dt}^T = \dfrac{\partial H}{\partial \lambda} \\ \dfrac{d\lambda}{dt}^T = -\dfrac{\partial H}{\partial \mathbf{x}} \end{cases} \tag{12}$$

and to the boundary conditions of the Euler-Lagrange equations, also called transversality conditions. For instance, we have the generic forms,

$$\pi_f(\mathbf{x}, \lambda; t_0) = \lambda(t_0) - \left(\frac{\partial J}{\partial \mathbf{x_f}} + \nu^T \frac{\partial \psi}{\partial \mathbf{x_f}} \right) \tag{13}$$

and because of the initial constraints we have the transversality condition at initial time t_L:

$$\pi_0(\mathbf{x}, \lambda; t_L) = \lambda_{\mathbf{V}}(t_L) + \nu_{\mathbf{0}} \frac{\Delta V_0}{\|\Delta V_0\|} \tag{14}$$

Note that $\lambda(t_L)$ is the initial condition and not completely defined, but it is guessed to such that the terminal constraints and the transversality conditions can be satisfied. Following calculus of variation theory and the Maximum Principle [9], the optimal control $\mathbf{u}^*(t)$ is the one minimising the Hamiltonian:

$$\mathbf{u}^* = \arg\min_{\mathbf{u}} H(\mathbf{x}, \lambda, \mathbf{u}; t)$$

and,

$$H(\mathbf{x}, \lambda, \mathbf{u}; t) = \lambda_{\mathbf{R}}(t)^T \mathbf{V_{sc}} - \lambda_{\mathbf{V}}(t)^T \frac{\mu \mathbf{R_{sc}}(t)}{\|R_{sc}(t)\|^3} + S(\mathbf{x}, \lambda, \mathbf{u}; t) \tag{15}$$

$$S(\mathbf{x}, \lambda, \mathbf{u}; t) = \frac{F_{Th}}{m_{sc}(t)} \mathbf{u}(t) \lambda_{\mathbf{V}}(t)^T - \lambda_m(t) \frac{F_{Th}}{g_0 I_{Isp}} \tag{16}$$

Clearly, the Hamiltonian is minimised for:

$$\mathbf{u}^* = -\delta(t) \frac{\lambda_{\mathbf{V}}}{\|\lambda_V\|}$$

with $0 \leq \delta(t) \leq 1$. As the control belongs to a compact set, and appears linearly in the Hamiltonian, it is in general bang-bang. In particular, S is called a switching function, and helps us choose at each time t, whether the control reaches its upper or lower bound ($\delta(t) = 1$ or $\delta(t) = 0$).

The optimal control is thus computed by minimising the Hamiltonian and solving a two point boundary value problem (TPBVP). Using a shooting method, the Euler - Lagrange dynamical equations are integrated using the initial conditions $[\mathbf{x}(t_L), \lambda(t_L)]$ while satisfying transversality conditions $\pi_f(\mathbf{x}, \lambda; t_0)$ and terminal constraints $\psi_f(\mathbf{x}; t_0)$. If $\mathbf{x}(t_L)$ is not completely defined, the missing elements have to be guessed, as for $\lambda(t_L)$. For instance, the decision vector $\chi(t_L)$,

$$\chi(t_L) = [\lambda_{R_0}, \lambda_{V_0}, \lambda_{m_0}, \mathbf{V_0}]$$

is used to satisfy the endpoint conditions. We now study 2 specific cases of deflection method. Each one has its own objective function, and requires a specific formulation.

Objective function 1: Impulsive Deflection

Using an impact strategy, the deflection formula in Eq.(4) can be reduced to the objective function of the Mayer form [6]:

$$J = K\frac{3av_{E,t_e}\sin\theta}{\mu}(t_e - t_0)\frac{m_{sc}(t_0)}{m_{sc}(t_0)+m_{ast}}\mathbf{U_{sc}}(t_0)\mathbf{v}_{ast}(t_0) \tag{17}$$

We denote with t_0 the time of impact, and with $\mathbf{U_{sc}}$ the spacecraft velocity relative to the asteroid. As $t_e - t_0 = \tau_s$ we will use this variable in the following developments. The terminal constraints for the position encounter are:

$$\psi_f(\mathbf{x}(t_0); t_0) = \mathbf{R}_{sc}(t_0) - \mathbf{R}_{ast}(t_0) \tag{18}$$

With the terminal constraints, the necessary conditions of optimality give the transversality conditions:

$$\begin{cases} \lambda_{\mathbf{V}}(t_0) = \dfrac{\partial J}{\partial \mathbf{V}_{sc}} \\ \lambda_{\mathbf{m}}(t_0) = \dfrac{\partial J}{\partial m_{sc}} \end{cases} \tag{19}$$

with,

$$\frac{\partial J}{\partial \mathbf{V}_{sc}} = K\frac{3av_{E,t_e}\sin\theta}{\mu}\tau_s\frac{m_{sc}(t_0)}{m_{sc}(t_0)+m_{ast}}\frac{\partial \mathbf{U_{sc}}(t_0)}{\partial \mathbf{V}_{sc}}\mathbf{v}_{ast}(t_0)$$
$$\frac{\partial J}{\partial m_{sc}} = K\frac{3av_{E,t_e}\sin\theta}{\mu}\tau_s\frac{m_{ast}(t_0)}{(m_{sc}(t_0)+m_{ast})^2}\mathbf{U_{sc}}(t_0)\mathbf{v}_{ast}(t_0)$$

As $m(t_L)$ and $\mathbf{R}(t_L)$ are imposed by the problem, the costates $\lambda_m(t_L)$ and $\lambda_{\mathbf{R}}(t_L)$ are free. Similarly, as there is already a constraint in the encounter position $\mathbf{R}(t_0)$, the associated costate $\lambda_{\mathbf{R}}(t_0)$ is also free. It is worth mentioning that the difference of order of magnitude between the asteroid mass and the spacecraft mass, allows to write,

$$\frac{m_{sc}}{m_{sc}+m_{ast}} \approx \frac{m_{sc}}{m_{ast}} \tag{20}$$

Assuming that the asteroid mass is much larger than the spacecraft mass,

$$\begin{cases} \lambda_{\mathbf{V}}(t_0) = -\alpha m_{sc}(t_0)\mathbf{v}_{ast}(t_0) \\ \lambda_{\mathbf{m}}(t_0) = \alpha \mathbf{U_{sc}}(t_0)\mathbf{v}_{ast}(t_0) \\ \alpha = K\dfrac{3av_{E,t_e}\sin\theta}{\mu}t_0\dfrac{1}{m_{ast}} \end{cases} \tag{21}$$

This shows, trivially, that to increase the deflection, in the fixed date problem we are considering, we need to increase either the spacecraft mass or the relative velocity at encounter.

Objective function 2: Continuous Deflection

Using a continuous deflection technique, such as a gravity tractor, the deflection formula can be simplified into:

$$J = \frac{3a}{\mu}v_{E,t_e}\sin\theta\int_0^{\tau_p}(\tau_s - \tau)\mathbf{v}_{ast}(\tau)\mathbf{A}(\tau)d\tau \tag{22}$$

We have to note that J depends only on the state of the spacecraft at the time of encounter with the asteroid. This is then a terminal function, of the Mayer form, and we have similar equations as for the problem 1 . We use rendezvous constraint between the spacecraft and the asteroid at t_0 :

$$\psi_f(\mathbf{x}(t_0); t_0) = \begin{bmatrix} \mathbf{R}_{sc}(t_0) - \mathbf{R}_{ast}(t_0) \\ \mathbf{V}_{sc}(t_0) - \mathbf{V}_{ast}(t_0) \end{bmatrix} \tag{23}$$

As done earlier, the optimality conditions for the given initial conditions are expressed by Eq.(19). As before, since $m(t_L)$ and $\mathbf{R}(t_L)$ are imposed by the problem, the costate $\lambda_m(t_L)$ and $\lambda_{\mathbf{R}}(t_L)$ are free. The encounter position $\mathbf{R}(t_0)$ is imposed by the asteroid state at terminal time, and thus the costate $\lambda_{\mathbf{R}}(t_0)$ is free. In the long duration thrust case, assuming that we thrust, at full throttle, in the direction of the asteroid velocity[6], we get:

$$J = \frac{3a}{\mu}v_{E,t_e}\sin\theta F_{Th}\int_0^{\tau_p}(\tau_s - \tau)v_{ast}(\tau)d\tau \tag{24}$$

Note that for a given date of encounter, J depends only on τ_p, which varies linearly with $m_{sc}(t_0)$ with the relation:

$$\tau_p = \frac{m_{sc}(t_0)}{q} \tag{25}$$

Also, as the integrand $(\tau_s - \tau)v_{ast}(\tau)$ is a positive quantity for all $\tau \in [0, \tau_p]$, J is a monotonic positive increasing function of τ_p. Consequently, the dates being fixed (e.g. encounter and impact dates), maximising J resumes to maximising $m_{sc}(t_0)$ and we may thus consider this case as a fixed times maximum final mass problem.

Case study: gravity tractor vs. kinetic impactor

We here consider as a study case a deflection mission to the asetroid 99942 Apophis, before the 2029 putative keyhole passage. We consider a spacecraft having an initial mass is 1500 kg. We aim at comparing, in this case, the performances of a gravity tractor strategy and those of a kinetic impactor. The spacecraft has 2 thrusters of thrust force $F_{Th} = 0.1$ N. The thruster specific impulse is chosen to be $I_{Sp} = 2500$ s. In the gravity tractor case, in conformity to the gravity tractor design proposed by Lu and Love [10] the spacecraft needs 2 thrusters of opposite cant angle. We suppose a cant angle of $\alpha_{cant} = 45°$, such that the acceleration applied on the asteroid is:

$$T_{max} = 2\frac{F_{Th}}{m_{ast}} \cos \alpha_{cant}$$

We use the results of the preceding sections to evaluate the deviation induced in both cases solving the fixed time optimal control problem grid sampling the departure and arrival dates. The spacecraft departure date and time of flight spaces are split into intervals of 50 days. The encounter date is 10694.5 MJD. The launch date varies between 7042 and 9964 MJD. The time of flight ranges from 1 to 3 years. The deflection is computed for every points on the grid. Due to the method and the optimisation technique, convergence is not guaranteed for every points on the grid. For instance, in the impact case the convergence rate is about 91 %, while in the gravity tractor case, as the terminal constraints are rendezvous constraints, the convergence is more difficult and the convergence rate reaches 75 %. When no convergence is possible, we set the deflection value to 0.

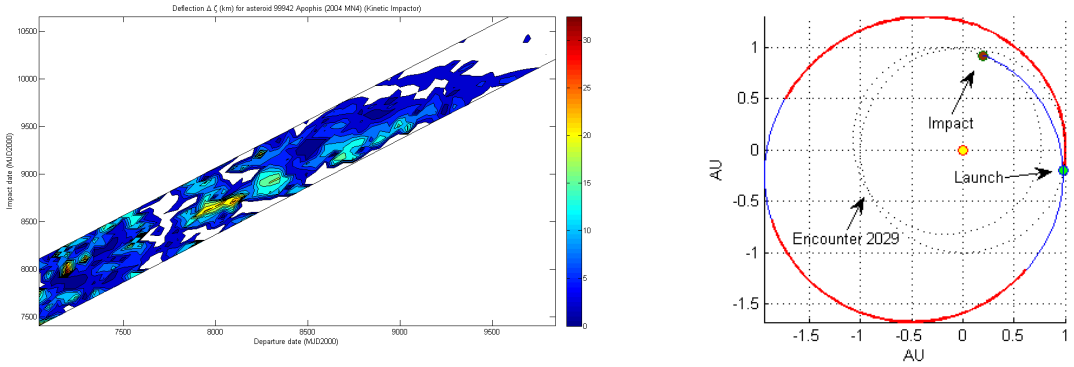

(a) Deflection achieved

(b) Best trajectory

Figure 4: Apophis: kinetic impactor capabilities

Figures 4 and 5 depict respectively the deflection map due to an impact on the asteroid, and the deflection map using a gravity tractor. What we can first infer from the figures is that the deflection is obviously not uniform on the time space. This is first due to the date at which the deflection technique start, as evident in the deflection charts presented in previous sections. In addition, even at a given encounter date with the asteroid, the deflection value changes because of the final spacecraft mass and, in general, of the encounter conditions. Opposite the previous studies, which did not account for the spacecraft mass and the inherent difficulty to place the spacecraft at the desired location and time, these graphs shows that to study a deflection technique efficiency, we have to take into account the initial phase of the mission, for instance the launch and the encounter problem. On figure 4, we notice that few launch dates allows to have an efficient deflection (the final word on the feasibility of the deflection would depend on how much deflection we actually need). Figure 4(b) represents the kinetic impactor trajectory that provides the highest deflection in the search domain. The spacecraft mass at impact is $1260kg$, the relative velocity is $5.2km/s$ and the spacecraft impact takes place 7.5 years before the Earth encounter. The impact geometry provides $\mathbf{U}\mathbf{v}_{ast} = 150km^2/s^2$, such that the impact energy is actually quite small and the deflection achieved by April 2029 is only $32.8km$.

On Figure 5, the different plot refer to different spacecraft dry mass and to the gravity tractor case. Once the spacecraft rendezvous with the asteroid, it still has to push to create the gentle push of the asteroid. As

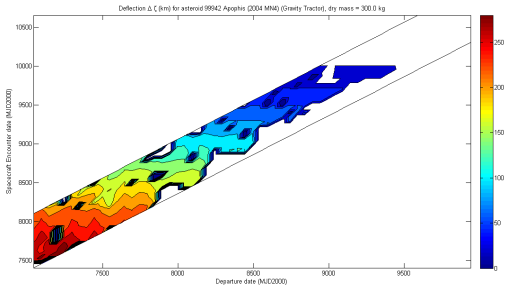

(a) Deflection achieved: dry mass 300 kg

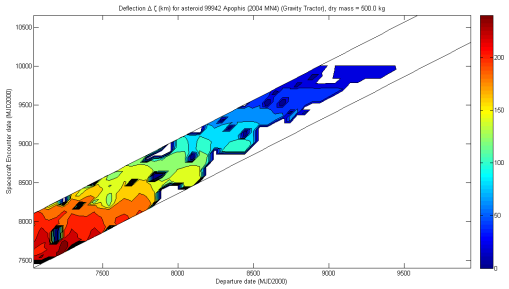

(b) Deflection achieved: dry mass 500 kg

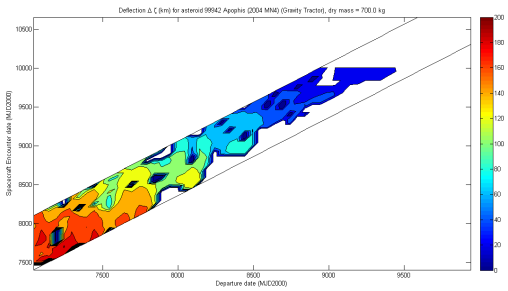

(c) Deflection achieved: dry mass 700 kg

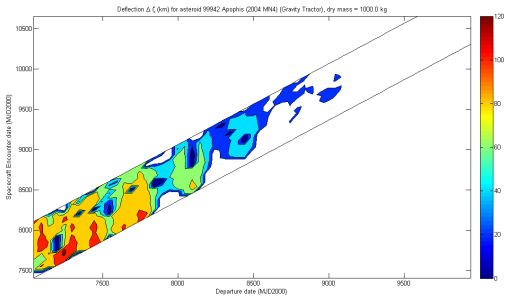

(d) Deflection achieved: dry mass 1000 kg

Figure 5: Apophis: Gravity Tractor capabilities.

in (4), the push time is limited by the available fuel mass, the spacecraft dry mass is an important design parameter as it affects heavily the achievable deflection. The fuel mass depends on the mass of the spacecraft at rendezvous with the asteroid, to which we should substract the dry mass of the spacecraft. The more dry mass we have, the less fuel remains. Consequently, as shown on figure 5, the performance of the deflection shrinks when the dry mass increases. An interpretation of the non convergence of trajectories with launch dates approaching the Earth encounter is that the condition of controllability imposes to have sufficient time for the spacecraft to reach the desired state. As a last remark we note that for this particular spacecraft design the gravity tractor technique seems to be very efficient with respect to the kinetic impactor. This fact is a direct consequence of the spacecraft design chosen and its validity is limited to the actual possibility of designing a spacecraft weighting 1500 kg and with engines able to have the quoted maximum thrust and specific impulse. The results here presented highlight the importance of accounting for the spacecraft design in a defection strategy trade-off. In particular, we may conclude that the two strategies considered may not be compared "in general" but only with respect to a given spacecraft (mass, thrust, specific impulse and minimum dry mass achievable).

Conclusion

We have studied common analytical estimates for the b-plane deflection due to impulsive and continuous deflection strategies, which shows how their extremely good accuracy fully justifies their extensive use in deflection studies. We have introduced the deflection charts as a preliminary tool to assess the threat of a given putative hazardous Earth encounter, explaining some counterintuitive choices for the start and push times. The deflection formula can be used as an objective function for interplanetary trajectory optimisation. In this case, the detailed study of the optimal control problem shows several new features of the design of deflection missions, including the bang-bang structure of the control and the importance of the Earth-asteroid phasing and of the spacecraft design in the evaluation of the deflection capabilities of a given strategy.

References

[1] D. Scheeres and R. Schweickart. The mechanics of moving asteroids. *2004 Planetary Defense Conference: Protecting Earth from Asteroids. AIAA paper 2004-1446*, 2004.

[2] T.J. Ahrens and A.W. Harris. Deflection and fragmentation of near-Earth asteroids. *Nature*, 360(6403):429–433, 1992.

[3] A. Carusi, G.B. Valsecchi, G. D'Abramo, and A. Boattini. Deflecting NEOs in route of collision with the Earth. *Icarus*, 159(2):417–422, 2002.

[4] R. Kahle, G. Hahn, and E. Kührt. Optimal deflection of NEOs en route of collision with the Earth. *Icarus*, 182(2):482–488, 2006.

[5] A. Rathke and D. Izzo. Keplerian consequences of an impact on an asteroid and their relevance for a deflection demonstration mission. *Proceedings of the International Astronomical Union*, 2(S236):417–426, 2007.

[6] D. Izzo. Optimization of interplanetary trajectories for impulsive and continuous asteroid deflection. *Journal of Guidance Control and Dynamics*, 30(2):401–408, 2007.

[7] J. Tschauner and P. Hempel. Rendezvous with a Target in Elliptic Orbit. *Astronautica Acta*, 11(5):104–109, 1965.

[8] R. Schweickart, C. Chapman, D. Durda, P. Hut, B. Bottke, and D. Nesvorny. Threat Characterization: Trajectory Dynamics. *NASA NEO Workshop*, 2006.

[9] L. S. Pontryagin, V. G. Boltyanskii, R. V. Gamkrelidze, and E. Mishchenko. *The mathematical theory of optimal processes (International series of monographs in pure and applied mathematics)*. Interscience Publishers, 1962.

[10] E.T. Lu and S.G. Love. Gravitational tractor for towing asteroids. *Nature*, 438(7065):177–178, 2005.